Rapid Communications

Kagome model for a $\mathbb{Z}_2$ quantum spin liquid

Matthew S. Block,[1] Jonathan D'Emidio,[2] and Ribhu K. Kaul[3]

[1]*Department of Physics and Astronomy, California State University, Sacramento, California 95819, USA*

[2]*Institute of Physics, Ecole Polytechnique Fédérale de Lausanne (EPFL), CH-1015 Lausanne, Switzerland*

[3]*Department of Physics and Astronomy, University of Kentucky, Lexington, Kentucky 40506-0055, USA*

(Received 18 June 2019; revised manuscript received 24 August 2019; published 9 January 2020)

We present a study of a simple model antiferromagnet consisting of a sum of nearest-neighbor SO(N) singlet projectors on the kagome lattice. Our model shares some features with the popular $S = 1/2$ kagome antiferromagnet but is specifically designed to be free of the sign problem of quantum Monte Carlo. In our numerical analysis, we find as a function of N a quadrupolar magnetic state and a wide range of a quantum spin liquid. A solvable large-N generalization suggests that the quantum spin liquid in our original model is a gapped $\mathbb{Z}_2$ topological phase. Supporting this assertion, a numerical study of the entanglement entropy in the sign free model shows a quantized topological contribution.

DOI: 10.1103/PhysRevB.101.020402

Quantum antiferromagnetism on the kagome lattice is an important playground in the study of quantum spin liquids emerging from frustrated magnetism. The most popular model in this family is the $S = 1/2$ kagome antiferromagnet $H = J\sum_{\langle ij\rangle}\vec{S}_i \cdot \vec{S}_j$. Despite a quarter of a century of intense research using an array of numerical and analytic methods on this important model the ground state of the $S = 1/2$ kagome antiferromagnet remains hotly contested. While the absence of magnetic order is uncontroversial [1–5], various nonmagnetic ground states have been proposed including, e.g., an array of quantum spin liquids (QSLs) [6–9] and valence bond solid ordering [1,10,11]. In parallel to the theoretical work, a number of synthetic quantum materials have been identified that provide venues where the interplay of quantum fluctuations and frustration on the kagome lattice give rise to novel unexplained behavior [12].

Of all the proposed phases of matter on the kagome, the so-called gapped $\mathbb{Z}_2$ quantum spin liquid [13] is the simplest example of an exotic state with long-range entanglement [14], a prototypical quantum state that cannot be deformed into a simple product or mean-field state. In its simplest incarnation, the excitations above the ground state come in two basic varieties, an e particle and an m particle which by themselves are bosons but are mutual semions [15,16]. Remarkably it has been shown that the presence of these excitations can be detected in the entanglement of the ground-state wave function itself, giving rise to a contribution called the "topological entanglement entropy" [17,18]. Although this state is not yet experimentally accessible, we now have a few model Hamiltonians that realize this topological order, including the toric code [19], the honeycomb Kitaev model [16], nonbipartite quantum dimer models [20,21], and models of frustrated bosons [22–24]. It is clearly of great interest to extend this family of models with an eye to finding simple models that could find realizations in physical systems.

Model. A number of variations on the basic $S = 1/2$ Heisenberg model have been introduced and studied on the kagome lattice, including Sp(N) [13], SU(N) [25], larger spin versions of the two spin Heisenberg exchange [26], as well as certain multispin interactions [27]. In this work we present and study a variant of the kagome antiferromagnet. Our model is constructed from generalized "spins" which commute on different sites and have a local Hilbert space of N states, denoted for site j as $|\alpha\rangle_j$ where $\alpha = 1, \ldots, N$. The Hamiltonian can be written simply as a sum of singlet projectors on the nearest neighbors of the kagome lattice,

$$H = -J\sum_{\langle ij\rangle} |S_{ij}\rangle\langle S_{ij}|, \tag{1}$$

$$|S_{ij}\rangle = \frac{1}{\sqrt{N}}\sum_{\alpha} |\alpha\alpha\rangle_{ij}. \tag{2}$$

Physically, the Hamiltonian Eq. (1) can be viewed as lowering the energy of singlet formation locally between nearest neighbors. Since all pairs of neighbors cannot simultaneously form singlets, quantum fluctuations play an important role in stabilizing the ground state. We note here that the usual $S = 1/2$ Heisenberg model is also a sum of singlet projectors, of the form Eq. (1) but with $|S_{ij}\rangle \to \frac{|\uparrow\downarrow\rangle - |\downarrow\uparrow\rangle}{\sqrt{2}}$, which aside from the crucial relative minus sign, is identical to our singlet Eq. (2) at $N = 2$. It is this discrepancy of sign that allows us to sidestep the infamous sign problem and carry out large volume numerical studies that are so far impossible for the $S = 1/2$ kagome Heisenberg model. The model, Eqs. (1) and (2), has a global SO(N) symmetry in which each site transforms in the fundamental representation, $|\alpha\rangle \to O_{\alpha\beta}|\beta\rangle$, and in the path integral can be interpreted as a statistical mechanics model of tightly packed unoriented loops [28]. A previous study [29] on the triangular lattice found a $\sqrt{12} \times \sqrt{12}$ valence bond solid order at large values of N. Here by introducing a solvable large-N limit and a numerical study of the entanglement entropy at finite N using an adaptation of a recently developed algorithm [30], we show that the increased geometric frustration of the kagome lattice realizes a $\mathbb{Z}_2$ topological quantum spin liquid.

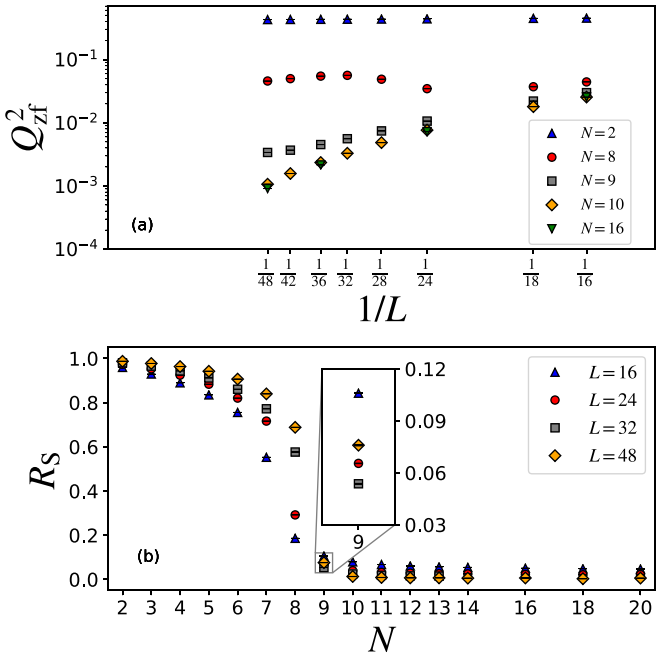

FIG. 1. Finite-size scaling of the quadrupolar order parameter for the model Eq. (1), shows the presence of long-range order for $N \leqslant 9$ and its absence for $N > 9$. The upper panel shows the $1/L$ scaling of the order parameter Q^2_{zf}. The lower panel shows the correlation ratio R_S as a function of N for different L. In the thermodynamic limit a value of 1 indicates long-range order, and 0 the absence of order. All values of N show R_S varying monotonically with increasing L except for $N = 9$. The inset shows the nonmonotonicity for $N = 9$, where for larger system sizes there is a trend of R_S to increase with L indicating quadrupolar long-range order.

We simulate the model Hamiltonian Eqs. (1) and (2), using the stochastic series expansion [31] with loop updates on $3 \times L \times L$ lattices at an inverse temperature β. To characterize the breaking of SO(N) symmetry we introduce the operator $\hat{Q}_{\alpha\beta} = |\alpha\rangle\langle\beta| - \frac{\delta_{\alpha\beta}}{N}$ which because of its tensorial nature we will call the "quadrupolar" order parameter. We refer to this state as "magnetic" because it breaks the internal SO(N) spin symmetry. The Fourier transformed susceptibility, $\chi_Q(\mathbf{k}) = \frac{1}{\beta N_{\text{site}}} \int_0^\beta d\tau \sum_{\mathbf{r}} e^{i\mathbf{k}\cdot\mathbf{r}} \langle Q_{\alpha\alpha}(\mathbf{r},\tau) Q_{\alpha\alpha}(\mathbf{0},0)\rangle$, is used to diagnose quadrupolar order. We define $Q^2_{\text{zf}} = \chi_Q(\mathbf{0})$ as the order parameter, a quantity which scales to a finite value in the thermodynamic limit in the quadrupolar phase and to zero otherwise. To facilitate detection of the long-range order, we also study a correlation ratio $R_S = 1 - \frac{\chi_Q(\mathbf{G}/L)}{\chi_Q(\mathbf{0})}$ where $\mathbf{G}$ is the shortest reciprocal lattice vector, which scales to 1(0) in the symmetry broken (unbroken) phase. As shown in Fig. 1, the quadrupolar order decreases as N is increased. Finite-size scaling shows that for $N \leqslant 9$ there is quadrupolar order that breaks the SO(N) symmetry and for $N > 10$ the quadrupolar order vanishes. The $N = 9$ case is on the verge of transition but a careful finite-size scaling indicates that it is quadrupolar ordered. We have searched extensively for translational symmetry breaking at the N for which quadrupolar order is absent (as was found in the triangular lattice [29]), but we find no evidence for this order, indicating the possibility of a quantum disordered state. We now present field theoretic arguments and numerical evidence that this phase is a $\mathbb{Z}_2$ quantum spin liquid.

Large-N limit. To introduce a solvable large-N limit that can capture both the quadrupolar as well as nonmagnetic phase, we generalize the spins in our model to transform under larger representations than the fundamental SO(N), using Schwinger bosons in which each local spin state is associated with one of N flavors of boson $b_{i\alpha}$ (with $[b_{i\alpha}, b^\dagger_{j\beta}] = \delta_{ij}\delta_{\alpha\beta}$). The generalized spin model is then

$$H_b = -\frac{J}{N} \sum_{\langle ij\rangle;\alpha,\beta} (b^\dagger_{i\alpha} b^\dagger_{j\alpha})(b_{j\beta} b_{i\beta}) \tag{3}$$

with the constraint $\sum_\alpha b^\dagger_{i\alpha} b_{i\alpha} = n_b$, which fixes the representation of the spin. Thus the family of models, Eq. (3), has two parameters n_b and N. Clearly $n_b = 1$ corresponds to Eq. (1). Increasing n_b is a generalization of Eq. (1), with different representations of SO(N). These are SO(N) analogs of the well-known Schwinger boson method of implementing higher representations of SU(N) [32,33].

Using boson coherent states we obtain a functional integral representation of the partition function $Z = \text{Tr}[e^{-\beta H_b}]$, with a field $\lambda_i(\tau)$ that enforces the on-site constraint and a Hubbard-Stratonovich field $Q_{ij}(\tau)$ that decouples the quartic interaction [32],

$$Z = \int D\lambda DQ e^{-\int d\tau \mathcal{L}_b}, \tag{4}$$

$$\mathcal{L}_b = \sum_{i,\alpha} [b^\dagger_{i\alpha} \partial_\tau b_{i\alpha} + \lambda_i (b^\dagger_{i\alpha} b_{i\alpha} - \kappa_b)] + \sum_{\langle ij\rangle;\alpha} \left(\frac{1}{J} |Q_{ij}|^2 + Q^*_{ij} b_{i\alpha} b_{j\alpha} + \text{c.c.} \right), \tag{5}$$

where we have set $n_b = \kappa N$. Integrating out the b fields we obtain an effective action proportional to N. By fixing κ a large-N limit can be accessed simply by a saddle-point evaluation. Assuming space and time independent Q and λ we find evaluating the trace over bosons, $Z = e^{-\beta V N f}$ (where V is the total number of spatial unit cells), where $f = \frac{1}{V} \sum_{\mathbf{k}\alpha} [\frac{zQ^2}{2J} - \lambda(\kappa + \frac{1}{2}) + \frac{1}{\beta} \ln 2 \sinh(\frac{\beta\omega_{\mathbf{k}\alpha}}{2})]$, and $\omega_{\mathbf{k}\alpha} = \sqrt{\lambda^2 - 4Q^2\gamma^2_{\mathbf{k}\alpha}}$ the dispersion of bosons and $\gamma_{\mathbf{k}\alpha}$ are the three modes $\alpha = 1, 2, 3$ of the adjacency matrix on the kagome, $\{1, \frac{1}{2}[-1 \pm \sqrt{3 + 2\cos(\vec{k} \cdot \vec{a}_i)}]\}$, where $\vec{a}_i$ are the three shortest lattice vectors on the triangular lattice Bravais lattice. At the saddle point (obtained by extremizing Q and λ), there are two phases: one where the b_α have a gap and the other where they are condensed. The condensed phase of the b_α breaks the SO(N) symmetry and corresponds to the quadrupolar order for the spin model; the implications of the gapped phase for the spin model are more subtle (we address them below). Numerically we find the transition between these two phases where the gap goes to zero is at $\kappa_c \approx 0.148\ldots$. This gives a phase boundary $n_b = \kappa_c N$ that we show in Fig. 2 as a solid line. Also shown in solid circles are the phases determined from quantum Monte Carlo (QMC) for $n_b = 1$. From this figure it is plausible by continuity that the quadruplar phase found in QMC corresponds to the condensation of b_α ($\kappa > \kappa_c$) and the liquidlike phase in the QMC corresponds to the state in which the b_α are gapped ($\kappa < \kappa_c$). We now ask what

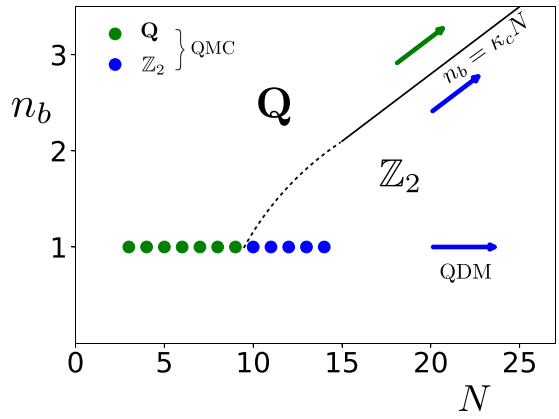

FIG. 2. The n_b-N phase diagram obtained for Eq. (3) from QMC and large-N limits: **Q** is for quadrupolar and $\mathbb{Z}_2$ is the topological spin liquid. The solid circles represent the QMC results from Fig. 1 for $n_b = 1$ which is identical to Eq. (1). The large-N Schwinger boson gives us the phase diagram when both $n_b, N \to \infty$, holding their ratio $\kappa = n_b/N$ fixed. At fixed $n_b = 1$ and large N a quantum dimer model (QDM) on the kagome lattice is obtained. The dashed line is a guide to the eye representing the simplest way the QMC and large-N results could be connected.

nonmagnetic state the original spin model goes into when the b_α acquire a gap. Following previous work [33], the state is determined by $1/N$ fluctuations beyond mean field, which take the structure of a U(1) gauge theory The unique aspect here is that because of the nonbipartite lattice all the b_i carry the same sign of gauge charge (as opposed to the staggered signs on bipartite lattices), and thus because of the structure of the saddle point there is a charge-2 Higgs field coupled to the U(1) gauge theory. As originally discussed in seminal work, such a Higgs phase leaves behind a $\mathbb{Z}_2$ gauge theory and a topological phase [34]. This line of argument was used previously to establish emergent $\mathbb{Z}_2$ gauge structures in large-N expansions [35]. We thus conclude that for $\kappa < \kappa_c$ the spin model will be in a $\mathbb{Z}_2$ quantum spin liquid phase. This suggests by continuity that the quantum disordered phase observed in our original model, Eq. (1) [the $n_b = 1$ limit of Eq. (3)] is also in this interesting phase. We test this conjecture below.

It is also possible to take a direct large-N limit of Eq. (1) (i.e., holding $n_b = 1$ fixed). Analogous to work on SU(N) models on bipartite lattices [36] we obtain as an effective theory, a quantum dimer model on the kagome lattice, where the spin wave function is obtained by replacing each dimer with $|S\rangle$ of Eq. (2). At $N = \infty$ all dimer coverings are degenerate and $1/N$ corrections introduce dynamics into the quantum dimer model. In this limit it is clear that quadrupolar order is absent, consistent with our numerical findings. While the quantum dimer model so obtained is not generally solvable, it is plausible that for $N \gg 1$, our model Eq. (1) ends up in the same $\mathbb{Z}_2$ spin liquid phase as an exactly solved kagome quantum dimer model [21], since the topological spin liquid is expected to be stable to all small deformations of the Hamiltonian. This limit suggests that at $n_b = 1$ the model remains in a liquid state for arbitrary large N, as shown in Fig. 2.

Entanglement. Having presented circumstantial evidence for a spin liquid in our model Eq. (1) from large-N expansions, we return to numerical simulations to provide direct evidence for the $\mathbb{Z}_2$ quantum spin liquid phase. We carry out measurements of the topological entanglement entropy (TEE), which has been a fruitful tool to detect topological order numerically [37–40]. In phases with topological order the TEE appears as a universal negative contribution to the entanglement entropy [17,18]. With L the linear size of a smooth simply connected subsystem, for large L in a thermodynamic system, $S_L = aL - \gamma + \ldots$, where the first term is the so-called "area law" contribution with a nonuniversal and the second term is the universal TEE piece. For the $\mathbb{Z}_2$ state found in our large-N study and in the kagome quantum dimer model, it is predicted that $\gamma = \ln(2)$ in the ground state. This expectation has been extended to finite temperatures as well, where due to two different excitation gaps associated with e and m particles, γ is predicted to show two plateaus at $\ln(2)/2$ and $\ln(2)$ as a function of inverse temperature for finite system size [41].

In order to isolate γ we compute the difference in entanglement entropy of differently shaped regions [17], written as $2\gamma = S^{(2)}_{\sqsubset} - S^{(2)}_{\square} + S^{(2)}_{\sqsupset} - S^{(2)}_{\sqsupset\sqsubset}$, where $S^{(2)}_A = -\ln(\mathrm{Tr}\rho^2_A)$ is the second Rényi entanglement entropy and the subscript A denotes the specific subsystem. Writing the Rényi entanglement entropy in terms of replica partition functions $S^{(2)}_A = -\ln(Z^{(2)}_A/Z^2)$ [42], the Levin-Wen measurement can be expressed as $\ln(Z^{(2)}_{\square}/Z^{(2)}_{\sqsubset}) - \ln(Z^{(2)}_{\sqsupset}/Z^{(2)}_{\sqsupset\sqsubset})$. To compute these partition function ratios numerically we have adapted a recently introduced algorithm [30] to the current problem. The method introduces a one-parameter family of partition functions $\mathcal{Z}^{(2)}_{AB}(\lambda)$ that interpolates between the two partition functions ($Z^{(2)}_A$ and $Z^{(2)}_B$) appearing in the ratio. In this extended ensemble the log ratio takes the form of a λ integral of a simple Monte Carlo estimator [43]. We have also tried other techniques to calculate the EE including the energy integration method [44] used in [38]; however, we find the current method to be better suited to our problem.

At large values of N and in the quantum spin liquid phase at the low temperatures of interest, it is difficult to efficiently sample our phase space using only traditional QMC loop updates. To improve the quality of our entanglement data we have incorporated annealing and replica exchange methods [43]. With these improvements we are able to measure γ reliably at moderately low temperatures, after which we encounter difficulties with equilibration and ergodicity. As we shall see, this allows us to observe the first plateau at $\ln(2)/2$ but not the second plateau at $\ln(2)$. Figure 3 shows the TEE as a function of inverse temperature β for the SO(N) model with $N = 8$ to $N = 11$ on an $L = 8$ lattice. As T is lowered, we clearly see a pronounced signal in the TEE for $N \geqslant 10$ near a plateau at $\ln(2)/2$. For $N \leqslant 9$, on the other hand, γ goes to zero in the low-temperature regime, consistent with the study of the quadrupolar order parameter shown in Fig. 1. Interestingly, even though for $L = 8$ the difference region in each ratio contains only $3 \times 2 \times 2$ we see reasonable quantization at the first plateau. To test how γ depends on system size L (with a corresponding scale up of the subsystem size) we present the SO(11) TEE data for $L = 8, 12, 16$ in Fig. 4. The data shows clear persistence of the $\ln(2)/2$ plateau,

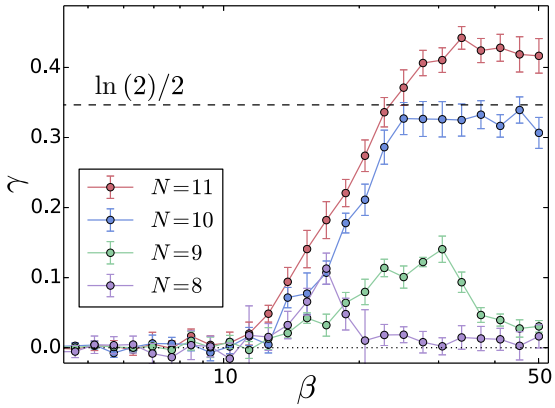

FIG. 3. The topological entanglement entropy γ of the model Eq. (1) for various values of N as a function of β for system size $L = 8$. A $T = 0$ quantized value of γ is indicative of topological order which clearly manifests itself for $N \geqslant 10$. For $N \leqslant 9$, the vanishing of γ is consistent with the appearance of quadrupolar order (see Fig. 1).

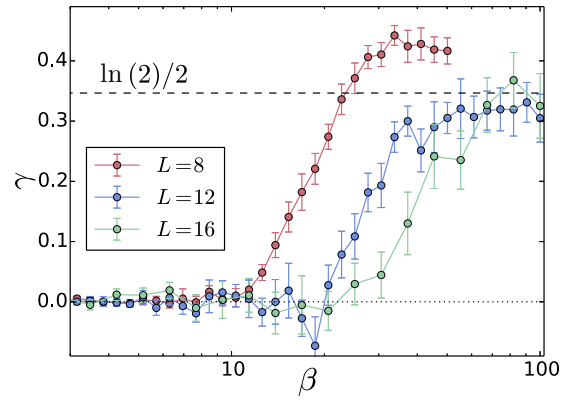

FIG. 4. The topological entanglement entropy γ as a function of β for $N = 11$ for $L = 8, 12, 16$. In the thermodynamic limit, we clearly see convergence to the first plateau of a $\mathbb{Z}_2$ spin liquid at $\ln(2)/2$. Another plateau at $\ln(2)$ is expected at still higher β.

the onset moving slowly to larger β as expected from the toric code [41]. We have also performed measurements at lower temperatures in an effort to see the second quantized plateau at $\ln(2)$ and despite signals that are consistent with this picture, proper equilibration here is challenging as is expected for a topological liquid with nonlocal excitations [43].

Outlook. We have unambiguously identified in sign-free Monte Carlo simulations, a $\mathbb{Z}_2$ quantum spin liquid in a simple two-site interaction model Eq. (1) of magnetism on a kagome lattice. Our work paves the way to study various interesting questions, including the nature of phase transitions out of the QSL, the role of isolated impurities, as well as the effect of large-scale disorder in QSLs. This simplicity of the model interaction, the exotic phase it hosts, and the absence of the sign problem make it a fundamentally interesting model of interacting quantum condensed matter. Apart from its theoretical interest, the simplicity of the model suggests it could be relevant for experiments as well. In cold atoms experiments, Mott insulating states with local Hilbert spaces size N as large as 10 have been realized with alkaline-earth-metal atoms [45], as well as kagome optical lattices [46]. In Mott systems with an N-fold Hilbert space there are two "most symmetric" interactions: the much studied permutation operator $\Pi_{ij} = \sum_{\alpha\beta} |\alpha\beta\rangle\langle\beta\alpha|$ (in the notation used in our Rapid Communication) and the projection operator $P_{ij} = \sum_{\alpha\beta} |\alpha\alpha\rangle\langle\beta\beta|$ that we discuss in our Rapid Communication, Eqs. (1) and (2). It is an exciting direction for future work to understand how these interactions can be controllably engineered with optical methods.

Acknowledgments. The computational work presented here was carried out using the XSEDE awards TG-DMR130040 and TG-DMR140061. Financial support was received through NSF DMR-1611161.

[1] J. Marston and C. Zeng, J. Appl. Phys. **69**, 5962 (1995).
[2] J. T. Chalker and J. F. G. Eastmond, Phys. Rev. B **46**, 14201 (1992).
[3] R. R. P. Singh and D. A. Huse, Phys. Rev. Lett. **68**, 1766 (1992).
[4] P. W. Leung and V. Elser, Phys. Rev. B **47**, 5459 (1993).
[5] P. Lecheminant, B. Bernu, C. Lhuillier, L. Pierre, and P. Sindzingre, Phys. Rev. B **56**, 2521 (1997).
[6] Y. Ran, M. Hermele, P. A. Lee, and X.-G. Wen, Phys. Rev. Lett. **98**, 117205 (2007).
[7] S. Yan, D. A. Huse, and S. R. White, Science **332**, 1173 (2011).
[8] Y. Iqbal, F. Becca, S. Sorella, and D. Poilblanc, Phys. Rev. B **87**, 060405(R) (2013).
[9] Y.-C. He, M. P. Zaletel, M. Oshikawa, and F. Pollmann, Phys. Rev. X **7**, 031020 (2017).
[10] P. Nikolic and T. Senthil, Phys. Rev. B **68**, 214415 (2003).
[11] R. R. P. Singh and D. A. Huse, Phys. Rev. B **76**, 180407(R) (2007).
[12] L. Balents, Nature (London) **464**, 199 (2010).
[13] S. Sachdev, Phys. Rev. B **45**, 12377 (1992).
[14] L. Savary and L. Balents, Rep. Prog. Phys. **80**, 016502 (2016).
[15] X. G. Wen, Phys. Rev. B **44**, 2664 (1991).
[16] A. Kitaev and C. Laumann, in *Exact Methods in Low-Dimensional Statistical Physics and Quantum Computing* (Oxford University Press, New York, 2008), Vol. 89.
[17] M. Levin and X.-G. Wen, Phys. Rev. Lett. **96**, 110405 (2006).
[18] A. Kitaev and J. Preskill, Phys. Rev. Lett. **96**, 110404 (2006).
[19] A. Kitaev, Ann. Phys. (NY) **303**, 2 (2003).
[20] R. Moessner and S. L. Sondhi, Phys. Rev. Lett. **86**, 1881 (2001).
[21] G. Misguich, D. Serban, and V. Pasquier, Phys. Rev. Lett. **89**, 137202 (2002).
[22] L. Balents, M. P. A. Fisher, and S. M. Girvin, Phys. Rev. B **65**, 224412 (2002).
[23] S. V. Isakov, Y. B. Kim, and A. Paramekanti, Phys. Rev. Lett. **97**, 207204 (2006).
[24] L. Dang, S. Inglis, and R. G. Melko, Phys. Rev. B **84**, 132409 (2011).
[25] P. Corboz, K. Penc, F. Mila, and A. M. Läuchli, Phys. Rev. B **86**, 041106(R) (2012).

[26] H. J. Changlani and A. M. Läuchli, Phys. Rev. B **91**, 100407(R) (2015).
[27] B. Bauer, L. Cincio, B. P. Keller, M. Dolfi, G. Vidal, S. Trebst, and A. W. W. Ludwig, Nat. Commun. **5**, 5137 (2014).
[28] R. K. Kaul, Phys. Rev. B **86**, 104411 (2012).
[29] R. K. Kaul, Phys. Rev. Lett. **115**, 157202 (2015).
[30] J. D'Emidio, arXiv:1904.05918.
[31] A. W. Sandvik, *Computational Studies of Quantum Spin Systems*, AIP Conf. Proc. No. 1297 (AIP, Melville, NY, 2010), p. 135.
[32] D. P. Arovas and A. Auerbach, Phys. Rev. B **38**, 316 (1988).
[33] N. Read and S. Sachdev, Phys. Rev. Lett. **62**, 1694 (1989).
[34] E. Fradkin and S. H. Shenker, Phys. Rev. D **19**, 3682 (1979).
[35] N. Read and S. Sachdev, Phys. Rev. Lett. **66**, 1773 (1991).
[36] N. Read and S. Sachdev, Nucl. Phys. B **316**, 609 (1989).
[37] S. Furukawa and G. Misguich, Phys. Rev. B **75**, 214407 (2007).
[38] S. V. Isakov, M. B. Hastings, and R. G. Melko, Nat. Phys. **7**, 772 (2011).
[39] T. Grover, Y. Zhang, and A. Vishwanath, New J. Phys. **15**, 025002 (2013).
[40] H.-C. Jiang, Z. Wang, and L. Balents, Nat. Phys. **8**, 902 (2012).
[41] C. Castelnovo and C. Chamon, Phys. Rev. B **76**, 184442 (2007).
[42] P. Calabrese and J. Cardy, J. Stat. Mech.: Theory Exp. (2004) P06002.
[43] See Supplemental Material at http://link.aps.org/supplemental/10.1103/PhysRevB.101.020402 for more details on the entanglement entropy measurements and the numerical algorithm used.
[44] R. G. Melko, A. B. Kallin, and M. B. Hastings, Phys. Rev. B **82**, 100409(R) (2010).
[45] M. A. Cazalilla and A. M. Rey, Rep. Prog. Phys. **77**, 124401 (2014).
[46] G.-B. Jo, J. Guzman, C. K. Thomas, P. Hosur, A. Vishwanath, and D. M. Stamper-Kurn, Phys. Rev. Lett. **108**, 045305 (2012).